

Journal of Materials Chemistry C

Accepted Manuscript



This is an *Accepted Manuscript*, which has been through the Royal Society of Chemistry peer review process and has been accepted for publication.

Accepted Manuscripts are published online shortly after acceptance, before technical editing, formatting and proof reading. Using this free service, authors can make their results available to the community, in citable form, before we publish the edited article. We will replace this *Accepted Manuscript* with the edited and formatted *Advance Article* as soon as it is available.

You can find more information about *Accepted Manuscripts* in the [Information for Authors](#).

Please note that technical editing may introduce minor changes to the text and/or graphics, which may alter content. The journal's standard [Terms & Conditions](#) and the [Ethical guidelines](#) still apply. In no event shall the Royal Society of Chemistry be held responsible for any errors or omissions in this *Accepted Manuscript* or any consequences arising from the use of any information it contains.



ARTICLE

Received 00th January 20xx,
Accepted 00th January 20xx

DOI: 10.1039/x0xx00000x

www.rsc.org/

Systematic Structure Modification of Low Bandgap Conjugated Polymer Improves Thin Film Morphology and Photovoltaic Performance by Incorporating Naphthalene in Side Chains

Ying Sun, Chao Zhang, Qizan Huang, Bin Dai, Baoping Lin*, Hong Yang, Xueqin Zhang, Lingxiang Guo, Yurong Liu

Abstract: In bulk-heterojunction (BHJ) polymer solar cell, film morphology of the active layer plays a significant role in determining the device performance. For lots of polymers, optimization of BHJ morphology can be achieved by employing high boiling solvent additives such as 1-chloronaphthalene (1-CN). However, the additive process significantly increases the device fabrication complexity and lead to poor reproducibility of device performance, which is not beneficial for large-scale manufacturing. In this paper, we show that well-organized film morphology can be achieved by systematic modification of the polymer structure. First, a new diketopyrrolopyrrole based monomer with the naphthalene group introduced to the terminal of alkyl side chain was synthesized. Naphthalene group was incorporated to improve the miscibility of the polymer with fullerene derivative and help the polymer chains self-assemble into ordered microstructure for defined film morphology. By simply varying the monomers' ratio in the copolymerization, we prepared a series of indacenodithiophene-diketopyrrolopyrrole based polymers namely, P1, P2, P3 and P4, with different content of naphthalene group functionalized side chains. The influences of naphthalene modification on the optical and electrochemical properties of polymers, film morphology and photovoltaic properties were investigated in details. As expected, we observed better miscibility without any significant effect on the electronic and optical properties of polymer for 25% molar percentage of naphthalene linked monomer employed during polymerization. However, further enhancement of the naphthalene content may decrease π - π stacking, hence leading to reduced optical property and hole mobility. When 50% molar percentage of naphthalene linked monomer was contained in polymerization, optimum device efficiency of 4.01% can be achieved, which was much higher than that of 2.92% for the 1-CN additive optimized non-naphthalene side chain counterpart based device.

1. Introduction

Organic photovoltaics have been attracting growing research interests due to their potentials for low-cost and fast roll-to-roll solution processability as well as their light weight and flexibility.¹⁻⁴ The majority of efficient organic solar cells to date were based on the bulk-heterojunction (BHJ) structure, in which an electron-donor polymer and an electron-acceptor fullerene derivative blended together to form the active layer.^{5,6} A PCE over 9% has been achieved in recent years for the most efficient polymer solar cell and efficiency of 15% or higher will be potentially achievable.⁷⁻⁹ Current research efforts have been directed to improve the processing feasibility and reduce the overall cost of the BHJ solar cells.

Film morphology of the BHJ active layer plays a critical role in determining the effectiveness of exciton dissociation, charge transport and charge collection, hence, the device efficiency.¹⁰

For BHJ solar cell, morphology optimization is even more difficult to be achieved because two components are involved and bicontinuous networks of donor and acceptor phases need to be formed for efficient charge transport and minimized charge recombination.^{11,12} To optimize the device performance, various approaches have been employed to manipulate the BHJ morphology and control phase separation.¹³ The most common and effective way is tuning the processing parameters including coating solvent, thermal annealing treatment, solvent annealing treatment, additives processing and substrate modification.^{14,15} However, the optimization is time-consuming and complex due to plenty of processing parameters. And largely different device efficiencies may be obtained for a given material depending on the processing condition.¹⁶ So developing polymers which can spontaneously form good film morphology when blending with fullerene derivatives is urgent for the further practical application of polymer solar cell.

In recent years, the electron-accepting diketopyrrolopyrrole (DPP) moiety has been widely in constructing donor-acceptor (D-A) type polymer due to its ease to synthesize, superior backbone planarity and good packing ability.

School of Chemistry and Chemical Engineering, Southeast University, Jiangning District, Nanjing 211189, Jiangsu Province, P.R. China.
Fax: 86-25-52090616; Tel: 86-25-52090616; E-mail: lbp@seu.edu.cn
See DOI: 10.1039/x0xx00000x

Variation of the comonomer unit has produced many polymers with extremely attractive optical properties, high charge mobility and photovoltaic properties.^{17, 18} However, for most of the DPP based polymers, optimization of film morphology is difficult to be completed and device fabrication often involves complex process methods including additive treatment and long term annealing. Incorporating high boiling additives such as 1,8-diiodooctane (DIO) and 1-chloronaphthalene (1-CN) in the blending solution is a widespread and effective approach to optimize the BHJ film morphology.¹⁴ However, due to its micro scale and high boiling liquid characteristic, the additive is not easy to control and need long term annealing and vacuum pumping to remove the additive after spin coating. Hence the complexity of device fabrication is greatly increased. Furthermore, the device efficiency reproducibility is low, probably because that the additive may still remain in some devices and consequently causes unfavourable interfacial contact.^{14, 19}

Previously, we synthesized a copolymer incorporating the indacenodithiophene (IDT) ring as donor unit and thiophene-flanked DPP moiety as acceptor unit.²⁰ Due to its immiscibility with PC₇₁BM, the polymer tend to phase segregate into large domain structures during the spin-coating process, leading to very poor device efficiency. In this paper, we tried to modify the polymer structure to manipulate the BHJ film morphology. Attempting to improve the miscibility with fullerene derivatives and induce spontaneous formation of good film morphology, we introduced naphthalene group to the side chains of polymer P1. First, a new DPP based monomer with the naphthalene group linked to be the terminal of side chain was synthesized. The content of naphthalene functionalized DPP monomer in the copolymerization was tuned. A series of polymers were prepared to systematically investigate the influence of naphthalene group modification on the optical and electrochemical properties of polymers, film morphology and photovoltaic properties. The results showed that improved film morphology and ease processability can be accomplished by the introduction of the naphthalene in the side chain. However, the bulky substituents gave rise to reduced structural order and π - π stacking and a trade-off must be achieved by controlling the content of naphthalene side chains in the polymer. BHJ solar cells fabricated from P3 with 50% molar percentage of naphthalene linked monomer contained in polymerization exhibited the optimum PCE reaching 4.01%, which was a substantial improvement over the PCEs of ca. 2.92% achieved by 1-CN additive optimized non-naphthalene polymer P1 based device.

2. Experimental part

2.1. Materials

3,6-Dithiophen-2-yl-2,5-dihydro-pyrrolo[3,4-c]pyrrole-1,4-dione (DPP) and 3, 6-bis-(5-bromo-thiophen-2-yl)-2,5-di-ethylhexyl-pyrrolo [3,4-c]-pyrrole-1, 4-dione (compound 4) were synthesized following the published reference.²¹ The synthesis of compound 5 was published before.²² All of the other chemicals used in this study were of analytical grade and

were purchased from Aladdin Reagent Co., Aldrich or TCI unless mentioned otherwise. Toluene was distilled from sodium under nitrogen atmosphere using benzophenone as an indicator. N, N-dimethylformamide (DMF) was dried over CaH₂ and distilled under vacuum.

2.2. Measurement and Characterization

¹H spectra were recorded on Bruker HW500 MHz spectrometer (AVANCE AV-500) in CDCl₃. Gel permeation chromatography (GPC) measurements were performed on a Waters 1515 chromatograph with a differential refractometer in room temperature with THF as eluent at a flow rate of 1 mL min⁻¹. UV-vis spectra tests were carried out using a ultraviolet spectrophotometer (UV-3600, Japan). The differential scanning calorimetry (DSC) was tested by TA instruments (SDT-Q600) under a heating rate of 10 °C min⁻¹ and a nitrogen flow of 50 mL min⁻¹. The thermogravimetry spectra were conducted using a thermo gravimetric analyzer (STA 409) under a heating rate of 10 °C min⁻¹ and a nitrogen flow of 100 mL min⁻¹. Cyclic voltammetries (CV) measurements were performed on a BAS CV-50W voltammetric system with a three-electrode cell in acetonitrile with 0.1 M of tetrabutylammonium hexafluorophosphate using a scan rate of 100 mV.s⁻¹ with ITO, Ag/AgCl and Pt mesh as the working electrode, reference electrode and counter electrode, respectively. AFM images were obtained on a Veeco multimode AFM with a Nanoscope III controller under tapping mode.

2.3. Synthesis of monomers and copolymers

2.3.1. Synthesis of Compound 1

A mixture of naphthol (2.8g, 20mmol) and K₂CO₃ (3.317g, 24mmol) in DMF (30ml) was stirred for 1h at room temperature and then 1,10-dibromodecane (32mmol) was added. After stirring overnight, the mixture was poured into water (200ml) and extracted with CH₂Cl₂. The organic phase was washed with dilute NaOH (3×100ml) and water (3×100ml), and then dried over Na₂SO₄. Purification on silica gel column chromatography provided compound 1 as white solid in 53% yield. ¹H-NMR (300 MHz, CDCl₃, ppm): δ = 8.25(m, 1H), 7.78(m, 1H), 7.50-7.32(m, 4H), 6.80(m, 1H), 4.12(t, 2H), 3.40(t, 2H), 1.80-2.0(m, 2H), 1.53-1.20(m, 14H).

2.3.2. Synthesis of Compound 2

Compound DPP (3.00g, 10 mmol) and anhydrous K₂CO₃ (4.15g, 30 mmol) were dissolved in DMF (100 ml) and heated to 120 °C for 2h. Then compound 1 (8.43g, 25 mmol) in 100 ml DMF was then added dropwise under N₂. After that, the mixture was further stirred and heated to 130 °C. After stirring overnight, the mixture was poured into water (400ml) and extracted with CH₂Cl₂, and then dried over Na₂SO₄. The crude product was purified by flash chromatography (petroleum ether/dichloromethane =5:1) to obtain compound 2 as brownish red solid in 54% yield. ¹H-NMR (300 MHz, CDCl₃, ppm): δ = 8.95(d, 2H), 8.30(m, 2H), 7.81(m, 2H), 7.65(d, 2H), 7.52-7.46(m, 4H), 7.44-7.32(m, 6H), 6.82(d,2H), 4.18-4.15(t, 4H),

4.12-4.08(t, 4H), 2.08-1.95(m, 4H), 1.78-1.72(m, 4H), 1.52-1.21(m, 18H), 0.89(t, 6H).

2.3.3. Synthesis of Compound 3

The compound 2 (0.864g, 1mmol) was dissolved in 50 ml CHCl_3 , to which N-bromosuccinimide (NBS) (0.41g, 2.3mmol) was added in the dark. After stirring at room temperature for 10h, the mixture was precipitated in methanol (200ml) to obtain the crude product. And then the residue was purified by column chromatography on silica gel (petroleum ether/dichloromethane=2:1 as eluent) to afford compound 3 as a shiny brown solid. Yield: 0.37g (92%). $^1\text{H-NMR}$ (300 MHz, CDCl_3 , ppm): δ = 8.92(d, 1H), 8.68(d, 1H), 8.30(d, 2H), 8.15(d, 2H), 7.65-7.48(m, 8H), 7.23(d, 1H), 6.98(d, 1H), 6.65(d, 2H), 4.14 (t, 4H), 4.08-3.98(m, 4H), 2.05-1.95(m, 4H), 1.92-1.85(m, 4H), 2.22(m, 4H), 1.52-1.21(m, 18H), 0.90(t, 6H).

2.3.4. Synthesis of Polymer

P1: A mixture of compound 5 (123.4 mg, 0.1 mmol) and compound 4 (68 mg, 0.1 mmol) in anhydrous toluene (5 ml) and DMF (0.5 ml) was carefully degassed three times before the addition of catalyst of $\text{Pd}_2(\text{dba})_3$ (4 mg) and $\text{P}(\text{o-tol})_3$ (10 mg). The resulting solution was heated to 110 °C and stirred under N_2 for 48h. Then the mixture was cooled down to room temperature and subsequently precipitated in methanol (200 ml). The polymer was collected by vacuum filtration and then purified by Soxhlet extraction with acetone and hexane. The obtained solid was dissolved in chloroform and then precipitation from hexane provided the polymer P1 as a dark black solid (79 %).

P2: P2 was synthesized from compound 5 (123.4 mg, 0.1 mmol), compound 4 (51 mg, 0.075 mmol) and compound 3 (26 mg, 0.025 mmol) using the same method as P2 with a yield (78 %).

P3: P3 was prepared from compound 5 (123.4 mg, 0.1 mmol), compound 4 (34 mg, 0.05 mmol) and compound 3 (52 mg, 0.05 mmol) using the same method as P3 with a yield (76 %).

P4: P4 was prepared from compound 5 (123.4 mg, 0.1 mmol), compound 4 (17 mg, 0.025 mmol) and compound 3 (78 mg, 0.075 mmol) using the same method as P4 with a yield (70 %).

2.4. Photovoltaic device fabrication

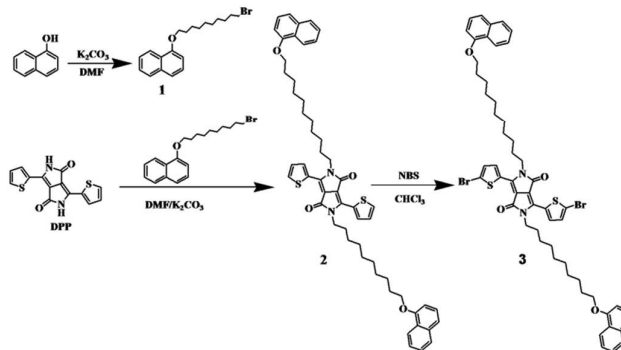
All the BHJ PSC devices were fabricated on indium tin oxide (ITO)-coated glass substrates, which were cleaned in advance by ultrason wave with detergent, deionized water, acetone, and isopropyl alcohol respectively for 20 min. PEDOT:PSS layer (~45 nm) was spin-coated from the its water solution (Baytron® PVP AI 4083, filtered at 0.45 μm) onto the ITO-coated glass and then baked at 150 °C for 10 min. The BHJ film was spin-coated in a nitrogen filled glove box from a blending solution of polymer with PC_{71}BM in o-DCB (with or without 1-CN additive) which was stirred overnight and filtered with a 0.2 μm PTFE filter. Subsequently, Ca (30 nm) and Al (100 nm) were thermally deposited successively under high vacuum ($< 2 \times 10^{-7}$ Torr) with a shadow mask to define the active area of the

devices (10.08 mm^2). J-V curves were measured under AM 1.5 G illumination with a Keithley 2400 SMU source measurement unit and an Oriel Xenon lamp (450 W). The device results have been calibrated by a standard silicon solar cell with a KG5 filter. Devices for the space-charge limited current (SCLC) mobility measurements were fabricated employing the same procedure with the photovoltaic devices except that the MoO_3 was deposited in replacement of Ca to produce hole-only devices.

3. Results and discussion

3.1. Design and synthesis of monomers and polymers

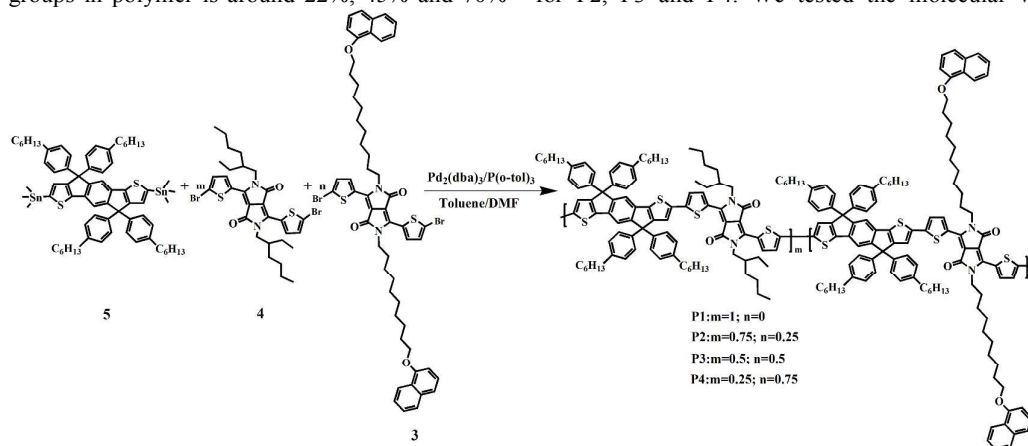
To investigate the influence of side chain modification on the polymer properties, the polymers were designed to possess the same polymer backbone but different side chains. We introduced the naphthalene groups to the polymer side chain in order to improve the miscibility of the polymer with fullerene derivatives. The content of naphthalene group functionalized side chain in the polymer was tuned by changing the monomer ratio in the polymerization. The effect of naphthalene group functionalization on the optical and electrochemical properties of polymers, film morphology as well as the solar cell device performance was investigated in details.



Scheme 1. Synthetic routes for the naphthalene group functionalized monomer

The synthesis route of the naphthalene group functionalized monomer is depicted in Scheme 1. The bromo terminated alkoxy naphthalene (compound 1) was synthesized according to the reported procedure²³ and the N-alkylation of DPP with compound 1 gave rise to compound 2. NBS bromination of compound 2 resulted in the brominated monomer (compound 3). The synthetic approaches for the polymers are illustrated in Scheme 2. Stille coupling polymerizations of the compound 3 and compound 4 with bis(trimethyltin) IDT donor monomer (compound 5) yielded a series of polymers by carefully changing the monomer ratio. These copolymers were purified by successive reprecipitation and Soxhlet extraction using acetone and hexane. The $^1\text{H-NMR}$ spectra of the polymers were shown in the supporting information. By comparing the relative integral values of the corresponding naphthalene protons' signal at around 8.23-8.35 ppm, 6.80-6.81 ppm to the DPP protons' signal at around 8.91 ppm, the content of

naphthalene groups in polymer is around 22%, 45% and 70% for P2, P3 and P4. We tested the molecular weight of the



Scheme 2. Synthetic routes for the polymers

Polymer	M_n [kg/mol]	PDI	Uv-vis Absorption				Cyclic voltammetry		Optical Bandgap (eV)
			in $CHCl_3$		In film		HOMO [eV]	LUMO [eV]	
			λ_{max} [nm]	λ_{onset} [nm]	λ_{max} [nm]	λ_{onset} [nm]			
P1	65.1	2.27	721	795	721	782	-5.26	-3.67	1.59
P2	24.4	2.83	721	793	721	820	-5.27	-3.76	1.51
P3	21.3	2.01	659	784	721	809	-5.28	-3.75	1.53
P4	19.8	1.86	639	770	659	814	-5.28	-3.76	1.52

Table 1. Molecular weights, optical and electrochemical properties of the polymers

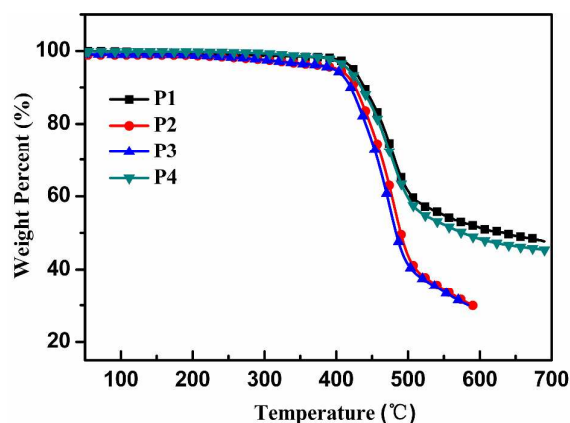


Figure 1. TGA thermograms of the polymers.

polymers by using gel permeation chromatography (GPC) using polystyrene as the standard and THF as the eluent. These copolymers had moderate number-average molecular weights of 19.8–65.1 kDa with a polydispersity index of 1.86–2.27 (Table 1). All of the resulted polymers have good solubility in common organic solvent such as chloroform, chlorobenzene and dichlorobenzene.

3.2. Thermal Properties of Polymers

Thermal properties of the copolymers were measured by using thermal gravimetric analysis (TGA). As depicted in Figure 1, the decomposition temperatures (T_d) with 5% weight loss were located at 423 °C, 415 °C, 390 °C and 416 °C for P1, P2, P3 and P4, respectively. The decreased T_d for the polymer P3 compared to P2 indicated that the naphthalene group may not be beneficial for the planar π - π stacking of polymer main chain. However, the fused naphthalene ring in the side chain can provide the noncovalent interactions with the polymer main

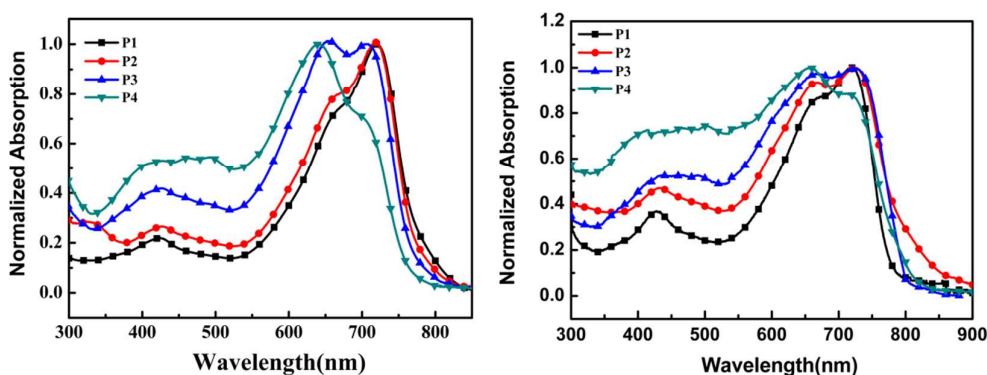


Figure 2. UV-vis absorption spectra of the polymers in chloroform (a) and in solid state (b).

chain and hence form the noncovalent crosslinking. With the greater content of naphthalene group, the noncovalent crosslinking degree increased and gave rise to improved thermal stability, which can probably be the reason for the enhanced Td for P4.²⁴ The excellent thermal properties of polymers can provide the superior stability of film morphology and prevent the degradation of device efficiency under high temperature, which is critical for the large scale application of polymer solar cells.²⁵

Neither melting point nor glass transition temperatures was observed from the differential scanning calorimetry DSC (see supporting information) measurements for all the polymers, indicating their amorphous characteristics. Furthermore, the results suggested that naphthalene group functionalization produced no significant effects on the thermal properties of polymers.

3.3. Optical and Electrochemical Properties of Polymers

Figure 2. shows the normalized UV-vis absorption spectra of the polymers in chloroform and in film. All the polymers exhibited two distinct absorption bands in the range of 350–800 nm, the one in longer wavelength band can be attributed to the intramolecular charge transfer (ICT) from the electron-rich IDT units to the electron-deficient DPP units and the one in the shorter wavelength band can be ascribed to be delocalized excitonic $\pi-\pi^*$ transition in the polymer chains.^{26, 27} In chloroform, polymer P2 showed the similar absorption spectra to polymer P1 with the same absorption maxima at 721 nm and only a slightly broadened wavelength band. For polymer P3, obvious band-broadening and a new shoulder peak appeared. With the further increased content of naphthalene group in the side chain, the shoulder peak at 721 nm gradually decreased for polymer P4 and the absorption hypsochromically shifted. This

observation suggested that the $\pi-\pi$ stacking may have been hindered by the introduction of the naphthalene group in the side chain.^{8, 28} The influence of the naphthalene group functionalization was also indicated in the solid state absorbance of the polymers by the gradually decreased absorption maxima at 721 nm and enhanced absorption peak at 659 nm with the increased naphthalene group content.

Comparatively, the thin films showed broader absorption bands compared to the absorption spectra in solution due to the stronger structural organization and more ordered packing in the solid state. Especially for the polymer P4, the shoulder peak in the longer wavelength was significantly enhanced in film compared to that in solution, suggesting the effect of naphthalene group on $\pi-\pi$ stacking can be partly relieved by the facile interchain organization in the solid state. Calculated from the onset of the UV-vis absorption in film, the bandgap of the polymer was determined as around 1.52–1.59 eV and the detailed data were listed in the Table 1.

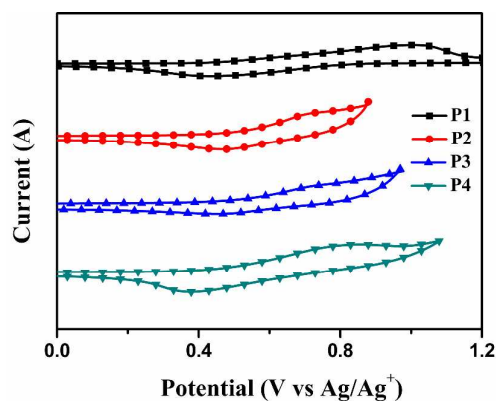


Figure 3. Cyclic voltammogram of the two polymers with a scan rate of 100 mV/s.



Journal of Materials Chemistry C

ARTICLE

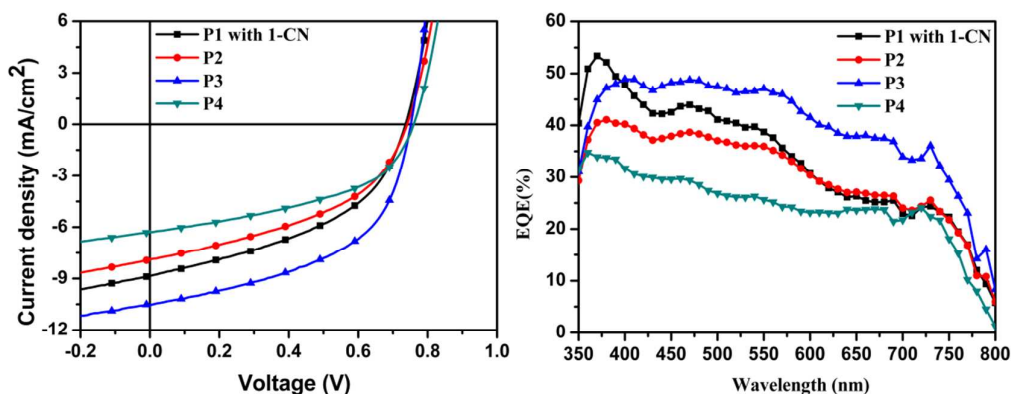


Figure 4. Respective J–V curves (a) and EQE curves (b) of optimized photovoltaic devices

Polymer	Blend Ratio	Solvent (V/V)	PCE (%)	V_{oc} (V)	J_{sc} (mA/cm ²)	FF (%)
P1	1:2	DCB	0.81	0.76	2.55	42.12
	1:3	DCB	0.95	0.77	2.63	47.21
	1:4	DCB	0.68	0.77	2.14	41.07
	1:2	DCB+4%1-CN	2.36	0.73	7.60	42.27
	1:3	DCB+4%1-CN	2.92	0.74	8.79	44.87
	1:4	DCB+4%1-CN	2.53	0.73	7.92	43.76
P2	1:2	DCB	2.55	0.74	7.84	43.95
	1:3	DCB	2.58	0.74	7.90	44.11
	1:4	DCB	2.42	0.74	7.56	43.22
P3	1:2	DCB	2.92	0.75	8.26	47.13
	1:3	DCB	4.01	0.75	10.46	51.11
	1:4	DCB	3.12	0.74	9.21	45.78
P4	1:2	DCB	2.10	0.75	5.77	48.53
	1:3	DCB	2.20	0.77	6.27	45.57
	1:4	DCB	2.17	0.76	6.12	46.69

Table 2. Photovoltaic parameters of the BHJ polymer solar cell

Cyclic voltammetry (CV) was employed to study the electrochemical properties of the polymers by using a Pt counter electrode and an Ag/Ag⁺ reference electrode in 0.1 M tetrabutylammonium hexfluorophosphate in acetonitrile with a scan rate of 100 mV s⁻¹. The cyclic voltammograms were shown in Figure 3 and the HOMO levels of polymers were calculated using the following equation:

$$\text{HOMO} = - [E_{ox} + 4.80] \text{ eV}$$

Here, E_{ox} is the onset of the oxidation potential. The measured results were calibrated using a ferrocene/ferrocenium redox couple. Since it was very difficult to get an obvious n-doping signal for the polymers, the n-doping process was not shown here. The LUMO levels were approximately evaluated by subtracting the optical band gap values from the corresponding HOMO levels. The polymers showed the similar HOMO and LUMO levels, which were determined as around

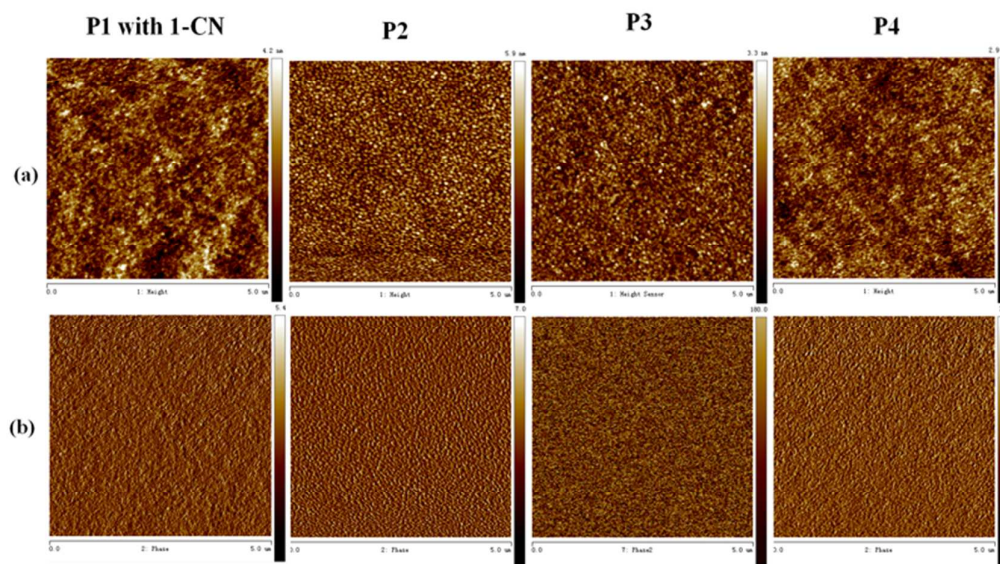


Figure 5. Tapping mode AFM height images (a) and phase images (b) of the optimized BHJ active layer based on polymer with PC₇₁BM (1:3)

-5.26 eV to -5.28 eV and -3.18 eV to -3.76 eV, respectively (Table 1). The relatively higher LUMO energy levels of the polymers compared to PC₇₁BM acceptor can ensure the energetically favorable electron transfer while the low HOMO levels of the polymers can provide sufficient air stability.^{29, 30}

3.4. Photovoltaic Properties of Polymers

The photovoltaic properties of the polymers were investigated by fabricating the conventional BHJ solar cell with the structure of ITO/PEDOT:PSS/polymer:PC₇₁BM/Ca/Al. Due to the better absorption ability of PC₇₁BM in the visible region compared to PC₆₁BM, we employed PC₇₁BM as the acceptor component in the BHJ active layer. The devices were characterized under simulated 100 mW.cm⁻² AM 1.5 G illumination and the representative current density–voltage characteristics of the optimized devices are depicted in Figure 4. The detailed processing method was illustrated in the experimental section and Table 2 summarized the device parameters in different processing conditions.

Weight ratio optimizations were conducted to achieve the well balanced charge carrier transporting. As indicated in Table 2, increasing the PC₇₁BM ratio from 1:1 to 1:3 gave rise to significant improvement in PCE for all the polymers. Due to the amorphous nature of the polymers and crystalline property of PC₇₁BM, more PC₇₁BM molecular was required to exclude from the polymer and form the bicontinuous conducting

network, which lead to the high optimum ratio of PC₇₁BM in BHJ film.^{13, 31} However, further enhancement of the PC₇₁BM ratio will lead to less polymer component in BHJ film and hence the light absorption property will be sacrificed. Consequently, decreased device performance was observed when the weight ratio varied from 1:3 to 1:4 for the polymers. Furthermore, the blend ratio in BHJ film can have effect on the intermediate charge transfer state between the exciton and free charges and consequently influenced the charge separation.³²⁻³⁴ So the FF and J_{sc} were strongly affected by the weight ratio.

Optimized photovoltaic device performances were obtained when the active layer was spin coated from o-DCB solution of the polymer and PC₇₁BM. Our previous results showed that polymer P1 based devices yielded very poor device efficiency due to the serious phase separation and large phase domain. To improve the film morphology, 1-chloronaphthalene(1-CN) was added into the o-DCB solution as the solvent additive to aid the miscibility of P1 with PC₇₁BM.³⁵ As shown in Figure 5, the tapping-mode atomic force microscopy (AFM) images indicated that smooth and homogeneous film of P1 and PC₇₁BM can be obtained employing the DCB:1-CN as the mixing solvent. Consequently, the optimized device performance based on P1:PC₇₁BM(1:3) was enhanced from less than 1% to 2.92%. However, device fabrication with the additive processing is very complex and the device efficiency reproducibility is not good.

To explore the effect of the naphthalene group functionalization of polymer on the BHJ film morphology and device efficiency, we fabricated the devices simply using the *o*-DCB as the solvent without any additive processing. *o*-DCB produced the optimum results probably because of that its relatively high boiling point can result in the low evaporation rate and hence provide extended evaporation time for the organization of polymer chains to yield optimum BHJ film morphology. Without the additive processing, polymer P2 based on device gave rise to the device efficiency of 2.58% although phase separation still can be observed from the AFM image of P2 based film with the surface roughness of 1.82 nm. With the increasing content of naphthalene group in the side chain, the AFM image of P3 based BHJ film featured a decreased phase separation and a smaller surface roughness of 1.15 nm. The photovoltaic device based on polymer P3:PC₇₁BM(1:3) showed a V_{oc} of 0.75 V, a J_{sc} of 10.46 mA /cm² and a FF of 51.11%, yielding an optimal PCE of 4.01%. The obvious trend of change in film morphology related to the increasing content of naphthalene group indicated that the introduction of naphthalene group in the polymer side chain was beneficial for the miscibility improvement of the polymer with PC₇₁BM.

In spite of the improved BHJ film morphology, polymer P4 based device exhibited a decreased PCE of 2.20% with a V_{oc} of 0.77 V, a J_{sc} of 6.27 mA /cm² and a FF of 45.57%. The reduced device efficiency can be ascribed to be the inferior packing ability of polymer P4 compared to P3. Furthermore, the BHJ film morphology for polymer P4 is quite homogeneous with the surface roughness only to be 0.69 nm. The fused naphthalene ring can form noncovalent interactions with the PC₇₁BM, which may make some PC₇₁BM be situated between the polymer chains. As a result, too many naphthalene group in the polymer side chain may hinder the formation of bicontinuous interpenetrating networks in the BHJ film and hence can give rise to reduced charge transport and lead to the decreased device efficiency of P4.^{36, 37}

In addition, the external quantum efficiency (EQE) wavelength dependencies of optimized photovoltaic devices based on polymer:PC₇₁BM (1:3) were measured and the EQE spectra were plotted in Figure 4 (b). The variation trend of the EQE responses is well consistent with that of the current density. Stronger EQE responses can be observed for polymer P3 compared to the other three polymers in the range of 300-800 nm. For the polymer P3, it possessed similar absorption bandgap and even broadened wavelength band compared to polymer P1. The enough content of naphthalene group in the side chain can provide the polymer P3 good miscibility with the PC₇₁BM and help the BHJ form good film morphology, which can facilitate more efficient charge dissociation and transport in active layer and hence lead to improved EQE and J_{sc} . Although the absorption intensity of polymer P4 increased at 300-600 nm, decreased absorption at 650-750 nm can be observed and the absorption hypsochromically shifted. Furthermore, the vanished shoulder peak indicated the hindered π - π stacking in polymer P4, which will probably lead to the inferior EQE.

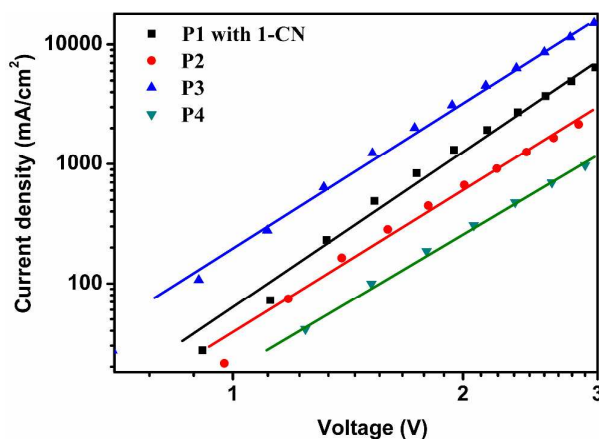


Figure 6. Current density and voltage (J-V) curves of the hole-only devices

To further investigate the effect of naphthalene group modification on the photovoltaic performance, the hole mobility of the polymer was measured by fabricating the hole only devices with the structure of ITO/PEDOT:PSS/Polymer:PC₇₁BM/MoO₃/Al. The J-V characteristics of the hole only devices were illustrated in Figure 6 and the hole transporting characteristic were modeled by the space charge limited current (SCLC) method using a field dependent mobility. The mobility values were extracted by modelling the dark current in SCLC region and calculated according to the following equation:

$$J = 9\epsilon_0\epsilon_r\mu V^2/8L^3$$

Here, J is the current density, ϵ_0 is the vacuum permittivity, ϵ_r is the relative permittivity of the polymer, μ is the hole mobility, and L is the thickness of active layer. The calculated hole mobility was 3.88 E-4, 3.35 E-4 cm² V⁻¹ s⁻¹, 8.21E-4 cm² V⁻¹ s⁻¹, 1.88E-4 cm² V⁻¹ s⁻¹ for P1, P2, P3 and P4, respectively. The low hole mobility of polymer P4 should be responsible for the decreased device efficiency compared to polymer P3. The hole only device results indicated that the introduction of the naphthalene group in the side chains had adverse effect on the packing ability of polymers. For polymer P3, the content of nap naphthalene group is high enough to achieve the good miscibility So regulate and control of the content of the naphthalene group is necessary for the device efficiency enhancement.

4. Conclusion

In summary, we presented a polymer structure engineering approach to improve film morphology and gain good device processability. A series of polymers P1, P2, P3 and P4 possessing the same indacenodithiophene-diketopyrrolopyrrole backbone but with different side chains have been synthesized through Stille coupling reaction. Instead of employing the 1-CN as the solvent additive, naphthalene group was incorporated in the polymer side chain to improve the miscibility of the polymer with fullerene derivative and help the BHJ spontaneously form good film morphology. The ease of

controlling the monomers' molar ratio in the copolymerization provided the opportunity to tailor the content of naphthalene group functionalized side chains. Thermal, optical and electrochemical properties, film morphology and photovoltaic performance of the four polymers were investigated and discussed in details. In agreement with our initial hypothesis, the naphthalene group in the polymer side chain can significantly improve the miscibility of the polymer with PC₇₁BM and hence increase the device efficiency. The UV-vis absorption indicated that the introduction of naphthalene group can lead to decreased molecular packing and nanostructural order. When 50% molar percentage of naphthalene linked monomer was introduced to the polymer, the PSC device based on P3 showed the optimum device efficiency of 4.01%. This result was much higher than that of 2.92% achieved by the non-naphthalene polymer based device which was optimized employing 1-CN solvent additive. This systematic investigation of structural effect on the film morphology and fundamental properties of polymer provides an different perspective to aid rational polymer design and practical application of BHJ PSCs.

Acknowledgements

The authors thank the National Natural Science Foundation of China (no. 21304018, 21374016), Jiangsu Provincial Natural Science Foundation of China (no. BK20130619, BK20130617) and Postdoctoral Research Funding Plan of Jiangsu Province (1302095C).

References:

- J. W. Chen and Y. Cao, *Acc. Chem. Res.*, 2009, **42**, 1709.
- Y. Y. Liang and L. P. Yu, *Acc. Chem. Res.*, 2010, **43**, 1227.
- A. J. Heeger, *Chem. Soc. Rev.*, 2010, **39**, 2354.
- P. L. T. Boudreault, A. Najari and M. Leclerc, *Chem. Mater.*, 2011, **23**, 456.
- J. E. Coughlin, Z. B. Henson, G. C. Welch and G. C. Bazan, *Acc. Chem. Res.*, 2014, **47**, 257.
- M. Pfannmoller, W. Kowalsky and R. R. Schroder, *Energy Environ. Sci.*, 2013, **6**, 2871.
- S. D. Dimitrov and J. R. Durrant, *Chem. Mater.*, 2014, **26**, 616.
- Y. Liu, J. Zhao, Z. Li, C. Mu, W. Ma, H. Hu, K. Jiang, H. Lin, H. Ade and H. Yan, *Nat. Commun.*, 2014, **5**, 5293.
- I. Etxebarria, J. Ajuria and R. Pacios, *Org. Electron.*, 2015, **19**, 34.
- F. Liu, Y. Gu, X. B. Shen, S. Ferdous, H. W. Wang and T. P. Russell, *Prog. Polym. Sci.*, 2013, **38**, 1990.
- J. E. Slot, X. He and W. T. S. Huck, *Nano Today*, 2010, **5**, 231.
- D. Bartsaghi, M. Turbiez and L. J. A. Koster, *Org. Electron.*, 2014, **15**, 3191.
- C. J. Brabec, M. Heeney, I. McCulloch and J. Nelson, *Chem. Soc. Rev.*, 2011, **40**, 1185.
- H. C. Liao, C. C. Ho, C. Y. Chang, M. H. Jao, S. B. Darling and W. F. Su, *Mater. Today*, 2013, **16**, 326.
- Z. Mao, T. P. Le, K. Vakhshouri, R. Fernando, F. Ruan, E. Muller, E. D. Gomez and G. Sauvé, *Org. Electron.*, 2014, **15**, 3384.
- C. R. McNeill, *Energy Environ. Sci.*, 2012, **5**, 5653.
- J. C. Bijleveld, V. S. Gevaerts, D. Di Nuzzo, M. Turbiez, S. G. J. Mathijssen, D. M. de Leeuw, M. M. Wienk and R. A. J. Janssen, *Adv. Mater.*, 2010, **22**, E242.
- A. P. Zoombelt, S. G. J. Mathijssen, M. G. R. Turbiez, M. M. Wienk and R. A. J. Janssen, *J. Mater. Chem.*, 2010, **20**, 2240.
- M. Jorgensen, K. Norrman, S. A. Gevorgyan, T. Tromholt, B. Andreasen and F. C. Krebs, *Adv. Mater.*, 2012, **24**, 580.
- Y. Sun, S.-C. Chien, H.-L. Yip, K.-S. Chen, Y. Zhang, J. A. Davies, F.-C. Chen, B. Lin and A. K. Y. Jen, *J. Mater. Chem.*, 2012, **22**, 5587.
- A. B. Tamayo, M. Tantiwivat, B. Walker and T. Q. Nguyen, *J. Phys. Chem. C*, 2008, **112**, 15543.
- Y. Sun, S. C. Chien, H. L. Yip, Y. Zhang, K. S. Chen, D. F. Zeigler, F. C. Chen, B. P. Lin and A. K. Y. Jen, *J. Mater. Chem.*, 2011, **21**, 13247.
- S. Sicard, J.-F. Bérubé, D. Samar, A. Messaoudi, D. Fortin, F. Lebrun, J.-F. Fortin, A. Decken and P. D. Harvey, *Inorg. Chem.*, 2004, **43**, 5321.
- Y.-S. Ye, Y.-J. Huang, C.-C. Cheng and F.-C. Chang, *Chem. Commun.*, 2010, **46**, 7554.
- M. Jørgensen, K. Norrman and F. C. Krebs, *Sol. Energy Mater. Sol. Cells*, 2008, **92**, 686.
- Y. Sun, S.-C. Chien, H.-L. Yip, Y. Zhang, K.-S. Chen, D. F. Zeigler, F.-C. Chen, B. Lin and A. K. Y. Jen, *J. Mater. Chem.*, 2011, **21**, 13247.
- P. M. Beaujuge, C. M. Amb and J. R. Reynolds, *Acc. Chem. Res.*, 2010, **43**, 1396.
- Y. L. Fan, B. P. Lin, Y. Sun, X. H. Gong, H. Yang and X. Q. Zhang, *Polym Chem-Uk*, 2013, **4**, 4245.
- T. M. Clarke and J. R. Durrant, *Chem. Rev.*, 2010, **110**, 6736.
- K. Akaike and Y. Kubozono, *Org. Electron.*, 2013, **14**, 1.
- J. A. Bartelt, Z. M. Beiley, E. T. Hoke, W. R. Mateker, J. D. Douglas, B. A. Collins, J. R. Tumbleston, K. R. Graham, A. Amassian, H. Ade, J. M. J. Frechet, M. F. Toney and M. D. McGehee, *Advanced Energy Materials*, 2013, **3**, 364.
- K. Vandewal, K. Tvingstedt, A. Gadisa, O. Inganas and J. V. Manca, *Nat. Mater.*, 2009, **8**, 904.
- D. Veldman, O. z. İpek, S. C. J. Meskers, J. r. Sweelssen, M. M. Koetse, S. C. Veenstra, J. M. Kroon, S. S. v. Bavel, J. Loos and R. A. J. Janssen, *J. Am. Chem. Soc.*, 2008, **130**, 7721.
- I. W. Hwang, C. Soci, D. Moses, Z. Zhu, D. Waller, R. Gaudiana, C. J. Brabec and A. J. Heeger, *Adv. Mater.*, 2007, **19**, 2307.
- J. R. Tumbleston, L. Yang, W. You and H. Ade, *Polymer*, 2014, **55**, 4884.
- S. Kwon, J. K. Park, J. Kim, G. Kim, K. Yu, J. Lee, Y.-R. Jo, B.-J. Kim, H. Kang, J. Kim, H. Kim and K. Lee, *J. Mater. Chem. A*, 2015, **3**, 7719.
- S. Nilsson, A. Bernasik, A. Budkowski and E. Moons, *Macromolecules*, 2007, **40**, 8291.